Holzforschung, Vol. 63, pp. 472–478, 2009 • Copyright © by Walter de Gruyter • Berlin • New York. DOI 10.1515/HF.2009.081

Neutron attenuation coefficients for non-invasive quantification of wood properties

David Mannes[1,2,*], Lidija Josic[2], Eberhard Lehmann[2] and Peter Niemz[1]

[1] Department of Civil, Environmental and Geomatic Engineering, Institute for Building Materials, Zurich, Switzerland

[2] Spallation Neutron Source (ASQ), Paul Scherrer Institute (PSI), Villigen, Switzerland

*Corresponding author.
Department of Civil, Environmental and Geomatic Engineering, Institute for Building Materials, ETH Zurich, 8093 Zurich, Switzerland
Phone: +41-44-632-3228
Fax: +41-44-632-1174
E-mail: dmannes@ethz.ch

Abstract

Attenuation coefficients and mass attenuation coefficients of wood were determined theoretically and experimentally for thermal and cold neutrons. Experiments were carried out at the neutron imaging facilities at the Paul Scherrer Institute, Villigen (CH). For the calculation of theoretical attenuation coefficients, only the three main elemental components (carbon, oxygen and hydrogen) were taken into consideration. While hydrogen accounts only for 6% (by wt) of wood, over 90% of the attenuation can be attributed to this element. Nitrogen and other trace elements were estimated to have a negligible impact on the theoretical attenuation coefficient. For the experimental determination of the attenuation coefficients, samples from different European and tropical wood species were tested in order to examine the influence of density and extractives content. Experimental results show a very strong linear correlation between attenuation coefficient and wood density irrespective of the tested species and extractives content that play only a minor role. As neutrons are very susceptible to scattering, it is necessary to apply a scattering correction if a quantitative evaluation is intended.

Keywords: neutron attenuation coefficients; non-destructive testing; quantification; wood properties.

Introduction

Transmission measurements based on electromagnetic radiation, such as γ- or X-rays have long been well established as non-destructive testing methods in the area of wood research (Bucur 2003a,b). A method working along similar principles is neutron imaging (NI), which represents an innovative technique for investigations on wood (Lehmann et al. 2001a; Osterloh et al. 2008). NI is complementary to X-ray methods and a very promising tool for a multitude of applications, such as quantitative evaluations of moisture contents (Niemz et al. 2002), the penetration behaviour of wood adhesives (Niemz et al. 2004) and conserving agents (Lehmann et al. 2005) or the determination of density profiles (Mannes et al. 2007). In order to exploit its full potential, it is necessary to consider the theoretical background of the method and to focus on the interactions between neutron radiation and wood on an elementary level. The attenuation coefficients and the mass attenuation coefficients are parameters describing those interactions and have already been determined for different energy levels of electromagnetic radiation based on theoretical or experimental data (Olson and Arganbright 1981; Liu et al. 1988; Hoag and Krahmer 1991). For NI on wood, however, those parameters have scarcely been scrutinised until now.

The aim of this study was to determine the attenuation coefficients and mass attenuation coefficients of wood for cold and thermal neutrons both theoretically and experimentally. The experiments were conducted at the neutron imaging beam-lines of the Paul Scherrer Institute (PSI), Villigen, Switzerland. European and tropical wood species with varying density and extractives contents were investigated.

Materials and methods

General principle

NI as well as X-ray imaging is based on transmission measurements, i.e., the degree to which an object within the beam path attenuates the incoming radiation (Figure 1) is observed. The result is a shadow image of the object yielding information on its inner structure and composition as the interactions between incoming beam and object depend on its elemental composition and density. Those interactions, which contribute to the attenuation in this type of experiment, comprise absorption and scattering.

How the atoms of different elements interact with the beam depends on the type of radiation. For example, X-ray photons interact with the electrons of atomic shells, resulting in a strong correlation between the atomic number and the interaction probability. The larger the atomic number, the higher is the interaction probability given by the microscopic cross-section, σ. Neutrons, on the other hand, possess a completely different interaction pattern with matter. Being electrically neutral particles, they are not likely to interact with electron shells of an atom. The interaction occurs with the atomic core itself and thus is not correlated with the atomic number. Instead, it shows a high interaction probability for some light elements, such as hydrogen, while heavier elements, such as lead, are practically transparent for neutrons.

The attenuation coefficient or macroscopic cross-section, Σ, is a parameter that describes the degree to which a certain material attenuates a beam. The attenuation results from all interactions of the beam with an object, which includes scattering as well as absorption. In a simplified first order approach, a

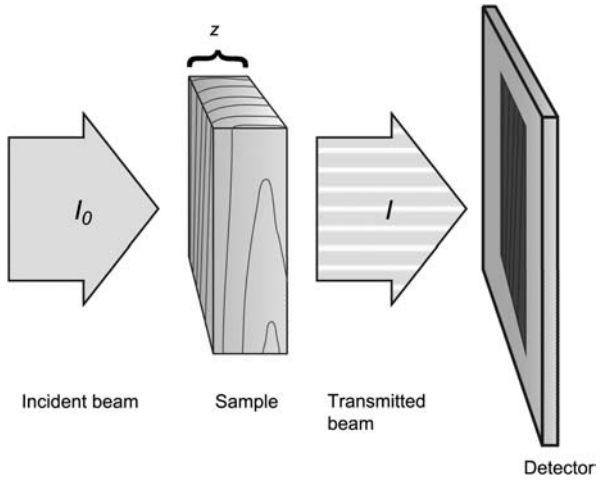

Figure 1 Simplified visualisation of the transmission measurement: the incident neutron beam with the intensity I_0 is led on a sample with the thickness z. The transmitted beam with the intensity I is registered with a 2D-detector.

differentiation between both interaction types can be neglected. The transmitted mono-energetic beam with energy E can be described by the linear attenuation law:

$$I(E) = I_0(E) \cdot e^{-\Sigma(E) \cdot z} \quad (1)$$

where I is the intensity of the transmitted beam, I_0 is the intensity of the incident beam, Σ is the neutron attenuation coefficient of the material and z is the specimen thickness. The linear attenuation law is valid under the assumptions that the beam is mono-energetic and that the thickness, z, tends towards 0.

The attenuation coefficient, Σ, comprises of the microscopic cross-section of an element, σ, i.e., the interaction probability of an element with the radiation, and the atomic density, N, of this element. For pure specimens of only one element, Σ is calculated as follows:

$$\Sigma = \sigma \cdot N. \quad (2)$$

For compound materials containing more than one element, the attenuation coefficients of the individual components sum to give the total attenuation coefficient of the sample:

$$\Sigma_{total} = \sum_{i=1}^{n} \Sigma_i = \sum_{i=1}^{n} (\sigma_i \cdot N_i). \quad (3)$$

The elemental composition of wood regarding the main components is relatively similar for all wood species (Rowell 2005). They only differ in the contents of some trace elements that are characteristic for the individual species. Thus, only the three main components, namely carbon (50%), oxygen (44%) and hydrogen (6%), were considered for the calculation of the theoretical attenuation coefficients while the other elements were neglected (% by wt).

Microscopic cross-sections, σ, of the individual elements were taken from data libraries (Pelowitz 2005). Those libraries provide energy dependent cross-sections for elements based on the free-gas model and also for a few elements bound in compounds. The σ-values for hydrogen, as bound in water, were taken into account, while for carbon and oxygen cross-sections of the free-gas model were used. As both utilised beam-lines show polychromatic characteristics, σ had to be calculated as a mean value weighted along the respective spectrum of each beam-line. The atomic density, N, was estimated according to Eq. (4):

$$N = (\rho/A) \cdot N_A, \quad (4)$$

where ρ is the material density, A the atomic weight and N_A Avogadro's constant.

For the calculation of the theoretical attenuation coefficient, a density of 0.6 g cm^{-3} was assumed.

The ratio of attenuation coefficient and density is called mass attenuation coefficient Σ/ρ. It is a material property specific to a certain neutron energy spectrum and a constant for all wood densities and wood species, as long as the actual elemental composition is similar to the assumed one.

Experimental setup

The experiments were carried out at the neutron imaging beam-lines NEUTRA and ICON at PSI, Villigen (CH). NEUTRA is a beam-line using neutrons within a thermal energy spectrum, while ICON provides a cold spectrum with less energetic neutrons. The characteristics of the two beam-lines have been described by Lehmann et al. (2001b) for NEUTRA and by Kuehne et al. (2005) for ICON. Figure 2 shows the spectra of the two beam-lines and the microscopic cross-sections, σ, of the elements taken into account for the calculation of the theoretical attenuation coefficients. Both facilities are provided with neutrons by the Spallation Neutron Source SINQ (Bauer 1998).

At both facilities, the setup for the described measurements was similar: the samples were positioned within the path of an almost parallel neutron beam in front of a detector. The detector was a scintillator-CCD camera system. The scintillator, doped with lithium or gadolinium as the neutron absorbing agent, converts the neutron beam into visible light. Within a light-tight box, the produced light is sent onto a CCD-camera via a mirror. The images were then digitally stored as 16-bit files.

Evaluation of the experimental data

Before the evaluation, the raw image data had to be processed in order to correct inhomogeneities of the experimental setup. First, a median filter was used on the images to eliminate "white-spots", which are outliers caused by such occurrences as direct hits of the CCD chip from γ-particles, for example. Then, the offset caused by the background noise of the CCD camera was subtracted from all of the images. In the next step, the images were flat-field corrected to reduce the impact of inhomogeneities of the beam and the scintillator. These standard steps are

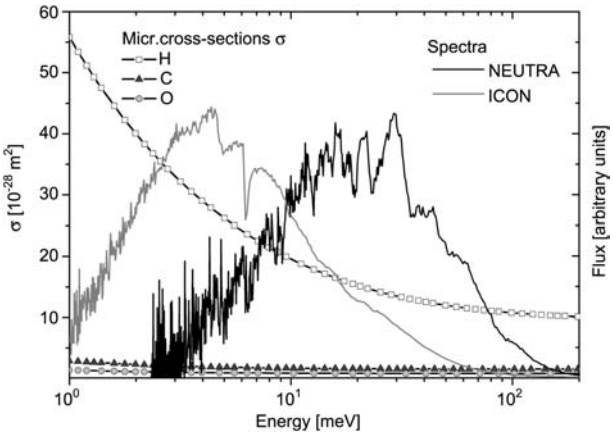

Figure 2 Energy spectra of the neutron imaging beam-lines NEUTRA (thermal spectrum) and ICON (cold spectrum) scaled on the right panel (normalised arbitrary units); the microscopic cross-sections of hydrogen (H), carbon (C) and oxygen (O) are scaled on the left panel; note the logarithmic scale of the X-axis.

common to all transmission based imaging methods, e.g., X-ray or synchrotron radiography and tomography.

As neutrons are susceptible to scattering, especially if hydrogen is involved, quantitative evaluation of the image data necessitates further corrections in particular for thick water layers and high amounts of moisture (Hassanein et al. 2005). Scattering events that can be problematic for the quantification of neutron images are caused by a combination of scattering within the sample and background scattering (Figure 3). Sample scattering can lead to an underestimation of the attenuation, because the scattered neutrons can deviate so that they hit the detector behind the sample. Thus, they are counted as a transmitted signal although they have interacted with the material and therefore should contribute to the attenuation. The background scattering consists of neutrons that are scattered back onto the detector by the experimental setup (e.g., facility's shielding material, camera box, …). The scattering corrections were performed by the software tool QNI (Quantitative Neutron Imaging) developed by Hassanein (2006). The software calculates the estimated contribution by scattering events and subtracts these from the neutron image. The estimation of the sample scattering is based on Point Scattered Functions (PScFs), which are calculated with Monte Carlo simulations. The PScFs "describe the scattering distribution caused by a neutron beam from a point source penetrating a material layer" (Hassanein 2006). It takes into account the energy spectrum of the used facility, the sample-detector distance, the elemental composition of the tested material, and the scintillator material used. All of these parameters have to be known in order to run the scattering simulation, on which the correction is based. An example of a typical transformation from raw image data to the final scattering corrected image is presented in Figure 4.

After correction, transmission values for each sample were derived from the corrected images using image-processing tools. With the obtained values, the attenuation coefficient, Σ, was calculated for each sample from Eq. (1):

$$\Sigma = \frac{-\ln T}{z}, \tag{5}$$

where T is the transmission of a sample with thickness z. The transmission, T, is defined as the ratio of the transmitted to the initial beam intensities:

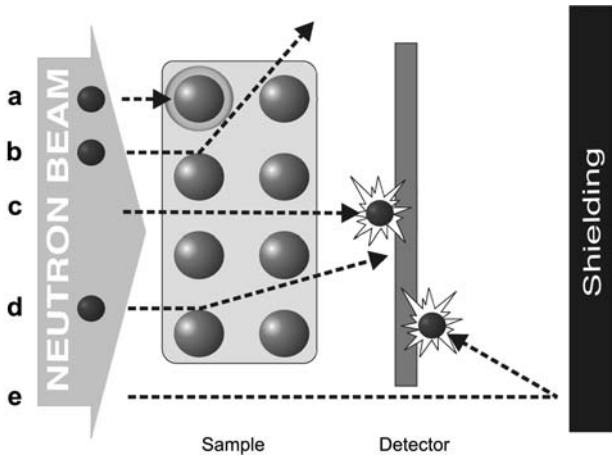

Figure 3 Simplified model of possible interactions between incident neutrons and the atoms within the object: (a) absorption, (b) scattering and (c) transmission; potential error sources for quantification: (d) sample scattering and (e) background scattering.

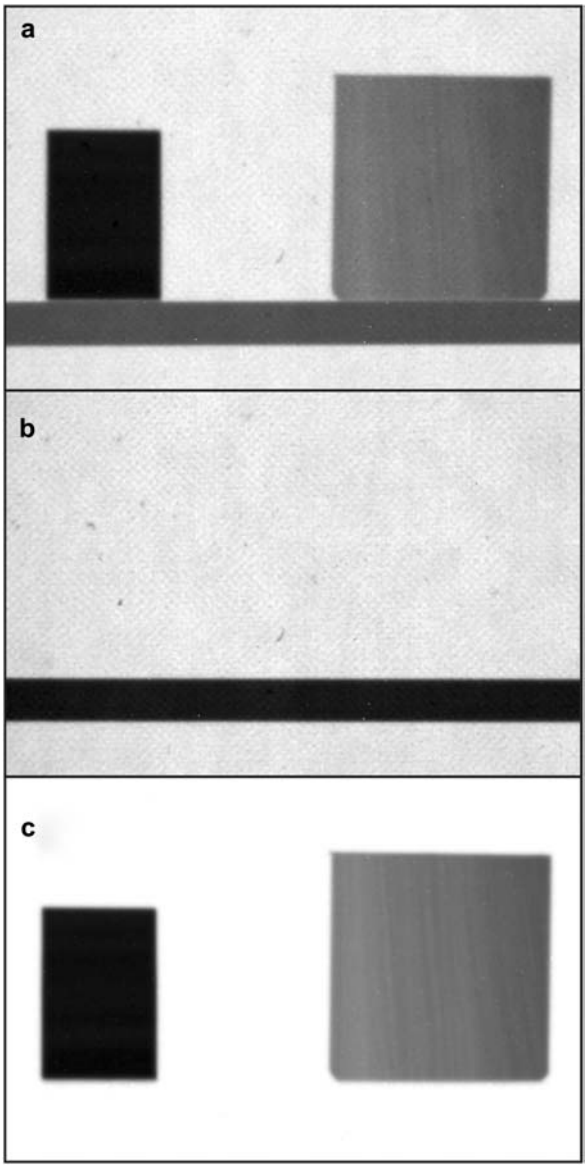

Figure 4 Correction of a typical neutron image (left: sample of Makassar ebony; right: sample of obeche). (a) The raw image, (b) the "flat field" without the samples, (c) the scattering corrected image.

$$T = \frac{I}{I_0}, \quad I = \int \Phi(E)\varepsilon(E)dE, \quad I_0 = \int \Phi_0(E)\varepsilon(E)dE, \tag{6}$$

where $\Phi(E)$ and $\Phi_0(E)$ are the beam energy distributions and $\varepsilon(E)$ is the energy dependent detector efficiency.

In addition, an error estimation for the Σ calculation was carried out including experimental uncertainties for I, I_0 and z.

Materials

The wood samples investigated cover a broad range of density and extractive contents (see Table 1, in which also the experimental setup is listed). All samples were oven-dried at 103°C until weight constancy before the actual experiments and the samples were stored within sealed plastic bags in an evacuated desiccator with silica gel. The dry samples were only unwrapped immediately before the measurements, which were started and concluded within a few minutes, to minimise the influence of water absorbed by the specimens. Although a small risk of some residual moisture after drying and water from post-drying sorp-

Table 1 Overview of the different experiments and utilised samples.

FACILITY (and objectives)	Species	Number of samples (*n*)	Dimensions (height×width×thickness) (cm)	Oven-dry density (g cm^{-3})
NEUTRA[a] and ICON[b] (Relation of attenuation coefficient or mass attenuation to density)	European beech	10	3×1.5×1.5	0.59–0.69
	Norway spruce	10		0.39–0.51
	Norway spruce (natural and artificially densified)	4 natural density	2×2×2	0.47
		4 densified	2×2×1.2	0.67–0.75
		4 densified	2×2×0.9	0.91–1.00
NEUTRA[a] (Relation of attenuation coefficient to extractives contents)	Norway spruce	2 untreated and 2 extracted[c] per species	2×2×1	0.39–0.42
	Common yew			0.56–0.63
	European larch			0.54–0.62
	Black locust			0.66–0.73
	Balsa	1 sample per species	5×2×2	0.2
	Obeche		2×2×1	0.3
	Merbau		2×2×0.6	0.9
	Makassar ebony		1×1.5×0.6	1.2

For Latin names of woods, see experimental section.
[a]NEUTRA (thermal spectrum), [b]ICON (cold spectrum), [c]Extraction: Tappi T 204 om-88 (modified) (Tappi 1988).

tion remains, the moisture content of the specimens was assumed to be zero. The sample size was selected such that sufficient transmission through the sample could be expected and inhomogeneities caused by factors, such as tree rings, could be compensated for.

In order to verify theoretical values, the first experiment performed with thermal and cold neutrons (NEUTRA and ICON) was focussed on the relationship of attenuation coefficient and mass attenuation with density. The wood species investigated comprised European beech (*Fagus sylvatica* L.) and Norway spruce [*Picea abies* (L.) Karst.]. Ten specimens per species were tested with their naturally varying densities and also a set of spruce samples was included with artificially modified density. The latter were cut from the same board, which was gradually densified in a press, resulting in samples with identical elemental composition but three different densities (uncompressed and two densification steps).

In the second experiment, the influence of the extractive contents on the attenuation coefficient was observed in addition to the density dependence. Two specimens from twin samples were scanned from the following species: Norway spruce [*Picea abies* (L.) Karst.], common yew (*Taxus baccata* L.), European larch (*Larix decidua* Mill.) and black locust (*Robinia pseudacacia* L.). The samples were cut from boards: one was extracted while the other one remained untreated. The extraction was carried out in an autoclave (2 h at 90°C and 2 bar) with ethanol-toluene as extractive agent according to the Tappi T 204 om-88 standard (modified) (Tappi 1988). This set of samples was measured with thermal neutrons (NEUTRA).

Together with the extracted samples, a smaller set of tropical woods was measured which had a broad natural range of densities and extractives contents. The species included balsa (*Ochroma lagopus* Sw.), obeche (or abachi or wawa) (*Triplochiton scleroxylon* K. Schum.), merbau (*Intsia* spp.) and Macassar ebony (*Diospyros* spp.).

Results and discussion

Theoretical attenuation coefficients

The theoretical attenuation coefficients and mass attenuation coefficients are listed in Table 2. Calculated atten-

Table 2 Theoretical microscopic cross-sections and attenuation coefficients for a simplified physical model of wood (density 0.6 g/cm^3) at the imaging beam-lines NEUTRA (thermal spectrum) and ICON (cold spectrum); only carbon, oxygen and hydrogen are taken into account as constituents.

		C	O	H	Wood
Material density, ρ	(g cm^{-3})				0.6
Relative fraction	(%)	50	44	6	
Number density, *n*	(cm^{-3})	1.51E+22	9.94E+21	2.17E+22	4.67E+22
Atomic weight, A	(g mol^{-1})	12	16	1	
Thermal neutron spectrum (NEUTRA)					
Microscopic cross-section, σ	(cm^2)	4.93E-24	4.00E-24	4.70E-23	
Attenuation coefficient, Σ	(cm^{-1})	0.07	0.04	1.02	1.13
Relative share of Σ	(%)	6	4	90	
Mass attenuation, Σ/ρ	(cm^2 g^{-1})				1.88
Cold neutron spectrum (ICON)					
Microscopic cross-section, σ	(cm^2)	5.29E-24	4.23E-24	6.02E-23	
Attenuation coefficient, Σ	(cm^{-1})	0.08	0.04	1.31	1.42
Relative share of Σ	(%)	6	3	91	
Mass attenuation, Σ/ρ	(cm^2 g^{-1})				2.37

uation coefficients, Σ, of the thermal and cold neutron spectra refer to absolutely dry wood with a density of 0.6 g cm^{-3}. Although hydrogen represents approximately only 6%$_{weight}$ of the wood substance, it accounts for 90% of the attenuation coefficients in the thermal spectrum and 91% in the cold spectrum. Carbon and oxygen, which contribute over 90% to the mass of wood, play only a minor role with regard to the attenuation of the neutron beam.

The mass attenuation coefficients Σ/ρ are constant and can be considered as wood properties for a certain energy spectrum. A comparison with the values determined by Olson and Arganbright (1981) shows that the mass attenuation coefficients for both neutron spectra (1.88 cm^2 g^{-1} for thermal neutrons and 2.37 cm^2 g^{-1} for cold neutrons) lay between the values of mono-energetic X-ray photons with 10 and 15 keV.

It should be restated that the presented theoretical attenuation coefficients represent only approximations of the real values as two assumptions had to be made for the calculation:

1) The first assumption concerns the elemental composition. While Olson and Arganbright (1981) also took nitrogen into consideration when determining the X-ray mass attenuation coefficients, it seemed negligible in the case of neutrons. For the calculation, only carbon, oxygen and hydrogen were taken into account. Nitrogen seemed negligible as it represents, together with all other trace elements, less than 1% (by wt) of wood. Besides the small content, nitrogen shows a small microscopic cross-section similar to that of carbon and oxygen.
2) The next assumption concerns the database for the microscopic cross-sections σ. The calculation is based on data retrieved from different data libraries, where the microscopic cross-sections for the different natural elements and isotopes are collected. Microscopic cross-sections for a certain element can vary significantly depending on whether the atom is considered as part of a compound or as a free atom. The σ-values are, e.g., 50% higher for hydrogen bound in water than for the free hydrogen. So far, no data are available for hydrogen, carbon and oxygen bound in cellulose, hemi-cellulose or lignin. While for hydrogen, the σ-values for hydrogen bound in water were used, but for carbon and oxygen the σ-values for their elemental form had to be applied.

The available cross-sections are given as energy dependent quantities. The experiments were carried out at facilities with two different polychromatic beams. For the calculation of the attenuation coefficients, the microscopic cross-sections were weighted against the corresponding spectra.

Experimentally determined attenuation coefficients

Part of the experiments is aimed at determining the relationship between attenuation coefficient and density, the impact of scattering, and the accordance of the experimental results with theoretical values. The results for the thermal spectrum are shown in Figure 5. The experimental attenuation coefficient, Σ, without scattering correction already shows a very strong linear correlation to the density but the difference to the expected theoretical values is very distinct. The data corrected with the scattering correction software, QNI, further increase the linearity of the results and the values are shifted very close to those of the theory. The corrected experimental data are in agreement to a great extent with the theoretical values as the correlation coefficient ($r^2 = 0.99$) determined by linear regression indicates. Figure 6 illustrates the mass attenuation coefficients, Σ/ρ, with and without scattering correction in comparison to the theoretical Σ/ρ-value. The mass attenuation, which should be constant, shows a considerable spread for the uncorrected data that are also quite low in comparison to the theoretical value. The scattering correction also has a clear influence on the mass attenuation by decreasing the spread of the results and by approaching the mean value of the experimental results to the theoretical one.

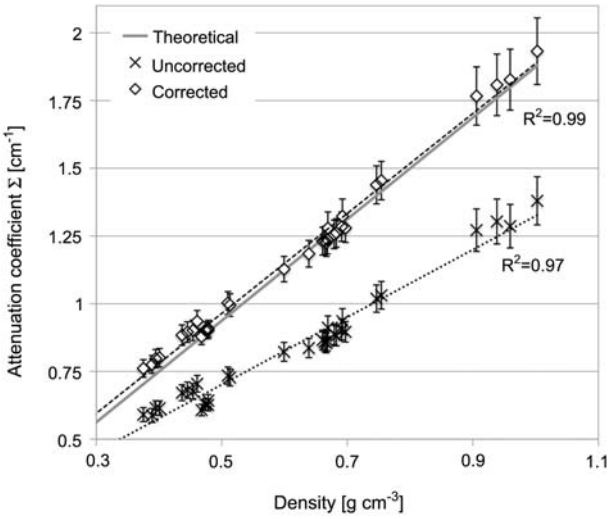

Figure 5 Attenuation coefficient Σ [thermal spectrum (NEUTRA)] of beech and spruce samples over the density; Σ without scattering correction: crosses; Σ with scattering corrections: rhombuses; theoretical values: grey line; vertical error bars: estimated measuring errors.

The experiment was repeated with identical samples for a cold neutron spectrum at the ICON facility. Figure 7 shows the results for attenuation coefficients over the density range. Similar to the experiment with the thermal

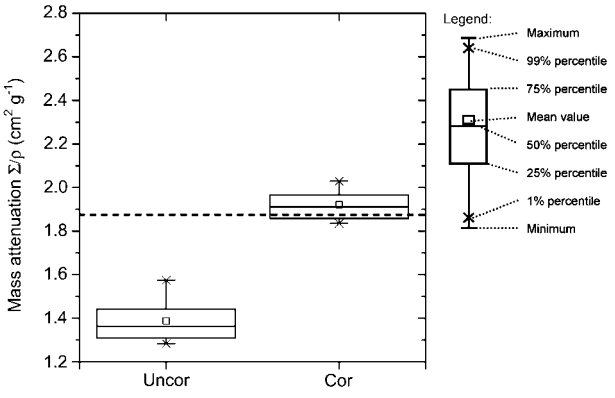

Figure 6 Mass attenuation coefficients (thermal spectrum) for the tested wood samples: experimental results without scattering correction (uncor), experimental results with scattering correction (cor) and the theoretical mass attenuation coefficient (dashed horizontal line).

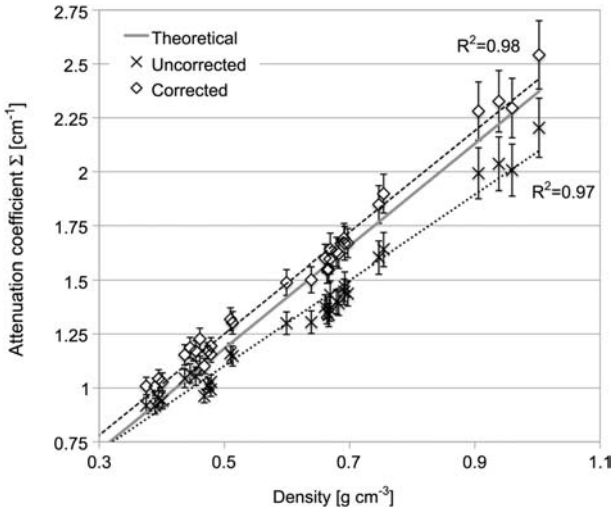

Figure 7 Attenuation coefficient Σ [cold spectrum (ICON)] of beech and spruce samples over the density; Σ without scattering correction: crosses; Σ with scattering corrections: rhombuses; theoretical values: grey line; vertical error bars: estimated measuring errors.

spectrum, a strong linear correlation with the density can be observed. However, unlike the first experiment, the uncorrected values already lie relatively close to the expected theoretical ones. The results with scattering correction are closer to the theoretical values, but not as close as for the thermal spectrum. Although the correlation is indubitable, it is not as pronounced as for the thermal spectrum. This tendency also appears in the mass attenuation coefficients (Figure 8). The uncorrected results are already in the vicinity of the theoretical ones showing that the scattering correction accounts for a smaller effect than for the thermal spectrum. Also, the spread of the uncorrected and corrected results is significant.

The differences in the results for thermal and especially cold spectra, when comparing the effect of the scattering correction can be ascribed to different effects. One could be that the scattering correction software was first developed for the NEUTRA beam-line. The interaction behaviour of neutrons in a thermal spectrum is well known and

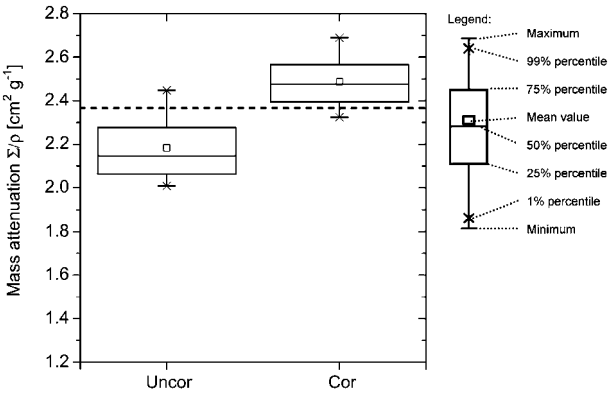

Figure 8 Mass attenuation coefficients (cold spectrum) for the tested wood samples: experimental results without scattering correction (uncor), experimental results with scattering correction (cor) and the theoretical mass attenuation coefficient (dashed horizontal line).

a multitude of empirical and theoretical data is available for this energy range. This is not the case for cold neutrons, which are used at ICON. As only very few facilities worldwide work with cold neutrons, fewer and less reliable information on that energy range is available. The higher discrepancy between theoretical and experimental data could indicate that the data used for the simulation of neutron scattering in the cold spectrum are not as reliable as those used for the thermal spectrum.

Another point that could add to the discrepancy between the beam-lines could be that the ICON beamline, which only came into operation at the end of 2005, was built with the experience gained at NEUTRA. Thus, some constructional weaknesses could be avoided, resulting in a possible overcompensation of presumed background scattering effects by the correction software.

Another part of the experiments aimed at ascertaining the possible influence of the extractives contents on the attenuation coefficient. Figure 9 shows the attenuation coefficients of the extracted and untreated wood samples for the thermal spectrum. A strong linear correlation is obvious between attenuation coefficient and density, and we suggest that the extractive content influences the attenuation coefficient only as far as it affects the density. This result confirms the working hypothesis at the beginning of the experiments as the influence of elements other than carbon, oxygen and especially hydrogen seems to be insignificant. Some of the values for the extracted samples in Figure 9 show higher values for the attenuation coefficient as well as for density. This is due to the fact that not all of the samples represent perfect twin samples with identical density and tree ring structure. Some of the samples had some knots leading to higher density and thus to higher attenuation in spite of the extraction.

The results obtained from the tropical wood species again show a high linear correlation between attenuation coefficient and density, which confirms the results of the other experiment as well as the theoretical considerations (Figure 10). When compared to the theoretical

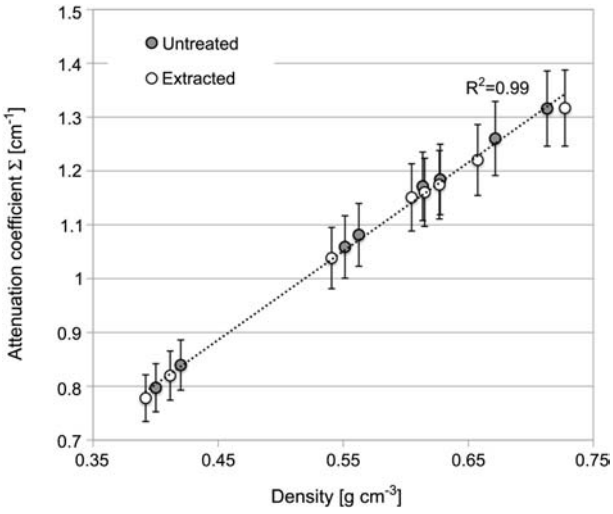

Figure 9 Attenuation coefficient Σ (thermal spectrum) of extracted (white) and untreated (grey) twin specimens of spruce, yew, larch and black locust over the density. Vertical error bars: estimated measuring errors.

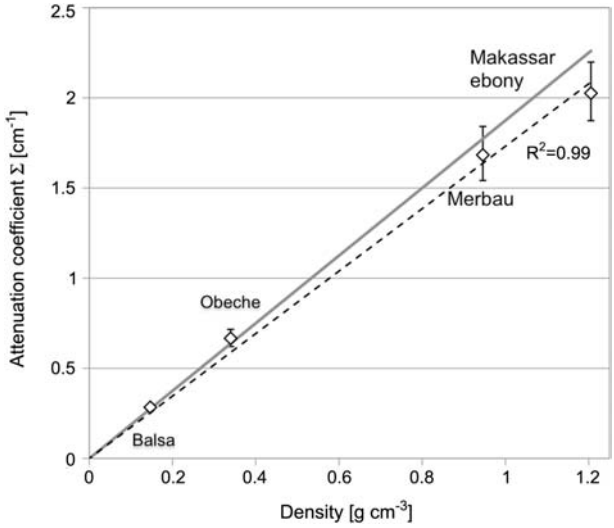

Figure 10 Attenuation coefficient Σ (thermal spectrum) of tropical wood species (balsa, obeche, merbau and Makassar ebony) over the density; vertical error bars: estimated measuring errors.

values, the results for the two species with higher densities (merbau and makassar ebony) lie below the calculated theoretical values. Possible explanations could be the very restricted number of samples tested in this experiment or the uncertainties of the scattering correction software. Nevertheless, the accuracy of the experimental results is satisfying as the theoretical values are still in the range of the estimated measuring error.

Conclusions

The attenuation coefficient of wood for thermal and cold neutron spectra shows a very strong linear correlation to the wood density unaffected by the tested wood species or extractive content. Although consisting only of approximately 6% of hydrogen, it accounts for 90% of the attenuation, while the other two main components, carbon and oxygen, account for the rest. For theoretical considerations of the attenuation coefficient of wood for neutrons, other elements can thus be neglected.

As neutrons are very susceptible to scattering, especially when interacting with hydrogen, correcting these scattering effects with suitable software (such as the QNI used) seems necessary if quantitative evaluations are intended.

The determination of the attenuation coefficients of wood is a necessary step towards utilisation of NI as a reliable non-invasive evaluation method in the field of wood research. It provides a framework for future experiments, which could focus on the distribution of density or especially of moisture. From the attenuation coefficients, measuring specifications regarding experimental setup, sample size and condition, etc. can be derived.

Acknowledgements

The authors want to thank Mr. M. Torres from Universidad Austral de Chile, Valdivia (Chile) for the extraction of the samples and Mr. T. Schnider and Dr. D. Keunecke for their help in the sample preparation.

References

Bauer, G.S. (1998) Operation and development of the new spallation neutron source SINQ at the Paul Scherrer Institut. Nucl. Instrum. Meth. B 139:65–71.

Bucur, V. (2003a) Techniques for high resolution imaging of wood structure: a review. Meas. Sci. Technol. 14:R91–R98.

Bucur, V. Non-destructive Characterisation and Imaging of Wood. Springer, Berlin, 2003b.

Hassanein, R. (2006) Correction methods for the quantitative evaluation of thermal neutron tomography. PhD thesis, ETH Zurich, Zurich.

Hassanein, R., Lehmann, E., Vontobel, P. (2005) Methods of scattering corrections for quantitative neutron radiography. Nucl. Instrum. Meth. A 542:353–360.

Hoag, M.L., Krahmer, R.L. (1991) Polychromatic X-ray attenuation characteristics and wood densitometry applications. Wood Fiber Sci. 23:23–31.

Kuehne, G., Frei, G., Lehmann, E., Vontobel, P. (2005) CNR – the new beamline for cold neutron imaging at the Swiss spallation neutron source SINQ. Nucl. Instrum. Meth. A 542: 264–270.

Lehmann, E., Vontobel, P., Scherrer, P., Niemz, P. (2001a) Application of neutron radiography as method in the analysis of wood. Holz Roh Werkst. 59:463–471.

Lehmann, E.H., Vontobel, P., Wiezel, L. (2001b) Properties of the radiography facility NEUTRA at SINQ and its potential for use as European reference facility. Nondestruct. Test. Eval. 16: 191–202.

Lehmann, E., Hartmann, S., Wyer, P. (2005) Neutron radiography as visualization and quantification method for conservation measures of wood firmness enhancement. Nucl. Instrum. Meth. A 542:87–94.

Liu, C.J., Olson, J.R., Tian, Y., Shen, Q.B. (1988) Theoretical wood densitometry: I – attenuation equations and wood density models. Wood Fibre Sci. 20:22–34.

Mannes, D., Lehmann, E., Cherubini, P., Niemz, P. (2007) Neutron imaging versus standard X-ray densitometry as method to measure tree-ring wood density. Trees – Struct. Funct. 21: 605–612.

Niemz, P., Lehmann, E., Vontobel, P., Haller, P., Hanschke, S. (2002) Investigations using neutron radiography for evaluations of moisture ingress into corner connections of wood. Holz Roh Werkst. 60:118–126.

Niemz, P., Mannes, D., Haase, S., Lehmann, E., Vontobel, P. (2004) Untersuchungen zur Verteilung des Klebstoffes im Bereich der Leimfuge mittels Neutronenradiographie und Mikroskopie. Holz Roh Werkst. 62:424–432.

Olson, J.R., Arganbright, D.G. (1981) Prediction of mass attenuation coefficients of wood. Wood Sci. 14:86–90.

Osterloh, K., Raedel, C., Zscherpel, U., Meinel, D., Ewert, U., Buecherl, T., Hasenstab, A. (2008) Fast neutron radiography and tomography of wood. Insight 50:307–311.

Pelowitz, D.B. (Ed.) MCNPX User's Manual, Version 2.5.0, LA-CP-05-0369. Los Alamos National Laboratory, 2005.

Rowell, R.M. (Ed.) Handbook of Wood Chemistry and Wood Composites. Taylor & Francis, Boca Raton, FL, 2005.

Tappi standard (1988) T 204. Om-88, Solvent extractives of wood and pulp.

Received October 27, 2008. Accepted February 19, 2009.
Previously published online May 7, 2009.